Physically Consistent Eddy-resolving State Estimation and Prediction of the Coupled Pan-Arctic Climate System at Daily to Interannual Time Scales Using the Regional Arctic Climate Model (RACM)

Wieslaw Maslowski
Naval Postgraduate School
Department of Oceanography
833 Dyer Rd.
Monterey, CA 93943
phone: (831) 656-3162 fax: (831) 656-2712 email: maslowsk@nps.edu

Andrew Roberts
Naval Postgraduate School
Department of Oceanography
833 Dyer Rd.
Monterey, CA 93943
phone: (831) 656-3267 fax: (831) 656-2712 email: afrobert@nps.edu

John Cassano
CIRES, University of Colorado at Boulder
216 UCB
Boulder, CO 80309
phone: 303-492-2221 fax: 303-492-1149 email: john.cassano@colorado.edu

Mimi Hughes
CIRES, University of Colorado at Boulder
and NOAA/ESRL/PSD R/PSD2
325 Broadway St.
Boulder, CO 80305
phone: 303-497-4865 fax: 303-497-6020 email: mimi.hughes@noaa.gov

Award Number: N00014-12-1-0419 / N00014-12-WX-21183

LONG-TERM GOALS

This project targets some of the key requirements in the Navy Arctic Roadmap 2014-2030 and in the 2014 Implementation Plan for the National Strategy for the Arctic Region, regarding the need for advanced modeling capabilities for operational forecasting and strategic climate predictions through 2030. The proposed research leverages ongoing developments of the state-of-the-art Regional Arctic System Model (RASM, previously called Regional Arctic Climate Model - RACM) through a multi-institutional program supported by the Department of Energy Regional and Global Climate Modeling (DOE/RGCM) program and two ongoing complementary projects. This project is aimed at improved modeling of the atmosphere-ice-ocean interface to advance representation of the past and present state

of the Arctic Climate System and prediction of its future states at time scales from daily (operational) through seasonal, interannual, and up to decadal (tactical). We use the Regional Arctic System Model (RASM) to extend the Navy sea ice predictive capability beyond the current forecasts of up to 7-day (provided by the Arctic Cap Nowcast/Forecast System (ACNFS) at NRL), to seasonal and up to decadal climate projections.

OBJECTIVES

Three main objectives are to (i) advance understanding and model representation of critical physical processes and feedbacks of importance to sea ice thickness and area distribution using a combination of forward modeling and state estimation techniques, (ii) investigate the relation between the upper-ocean heat content and sea ice volume change and its potential feedback in amplifying ice melt, (iii) upgrade RASM with the above improvements to advance both operational and tactical prediction of arctic climate using a single model.

APPROACH

We use the Regional Arctic System Model (RASM; *Maslowski et al.* 2012), which is a fully coupled, limited-area model (Figure 1) that includes the Weather Research and Forecasting (WRF) atmospheric model, optimized for polar regions and the Variable Infiltration Capacity (VIC) model representing land surface and hydrological processes. The Parallel Ocean Program (POP) and Community Sea Ice Code (CICE) models are regional versions of those used in CESM. These four components are coupled using the CESM coupler, CPL7. The model domain covers the entire pan-Arctic region and includes the whole marine cryosphere of the Northern Hemisphere.

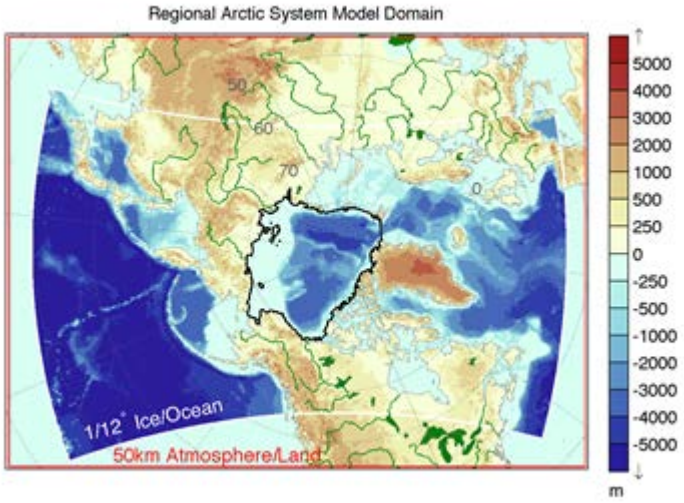

Figure 1. Configuration of the Regional Arctic System Model. The 1/12˚ ocean-ice domain (white boundary) includes the maximum sea ice zone relevant to the Arctic. The 50-km atmosphere-land domain (red boundary) includes the Arctic System watershed (major inland waterways in green). Shading represents model topography and bathymetry. The area encircled by the black line represents the central arctic analysis domain.

For parameter sensitivity studies discussed below we have used a subset of the fully coupled RASM model (G-compset), where WRF and VIC have been replaced with prescribed reanalysis data. To explore the sensitivity of RASM to the strength of atmospheric constraint, we perform two RASM simulations with and without spectral nudging in WRF with the WRF Four-dimensional Data Assimilation (FDDA) package. Using FDDA allows us to tightly constrain RASM-WRF by its atmospheric reanalysis boundary conditions (currently ERA Interim), which already include direct data assimilation of a very large quantity of observations (i.e., satellite radiances, radiosondes, etc). Although a few recent publications have investigated the impact of WRF FDDA nudging (which includes grid nudging and spectral nudging) on regional climate simulations (Bowden et al. 2012; Liu et al. 2012), testing of WRF FDDA within a fully coupled system like RASM has not been performed. Further, while a few studies have found that nudging of regional climate models is perhaps necessary to prevent circulation biases from developing, these studies have focused neither on the impact these circulation biases have on other components of the system (e.g., sea ice), nor the numerical and physical reasons these biases develop in the first place.

WORK COMPLETED

Spectral nudging in RASM-WRF

The PIs at the University of Colorado tested RASM's sensitivity to WRF run with and without FDDA nudging. The nudged simulation (RASM_nudg) was configured to optimally constrain the circulation, by nudging both meridional and zonal wind as well as temperature, from approximately 500 hPa to the top of the model, with nudging strength increasing with altitude. The RASM simulation with nudging turned off (RASM_nonudg) doesn't use the FDDA package in WRF at all, although the WRF domain is still constrained at its lateral boundaries by ERA Interim.

Without data assimilation, RASM's atmosphere develops large circulation biases. These biases are largest far from the surface: For example, Figure 2 shows mean 500 hPa geopotential height (GPH) contours in ERA Interim, RASM_nudg, and RASM_nonudg. In winter, RASM_nudg's circulation patterns match those in reanalysis almost identically, whereas RASM_nonudg has far too high GPH in the central Arctic and over northern Canada and Greenland. In summer, biases in RASM_nonudg's circulation aloft are not as large, but are still improved in RASM_nudg. These large biases aloft manifest themselves as large circulation biases at the surface (Fig. 3). Wintertime sea level pressure (SLP) contours align closely in RASM_nudg and ERA Interim, whereas in RASM_nonudg, the Aleutian low is shifted westward from its proper climatological position, the Beaufort high extends Arctic, and the Icelandic low is very weak and shifted eastward from its proper location. Summer SLP biases in RASM_nonudg are smaller than winter SLP biases, but are still substantial, and are again greatly improved in RASM_nudg. Although the magnitude of SLP biases is somewhat smaller than the biases aloft, SLP biases still have important consequences for sea ice drift and surface temperatures.

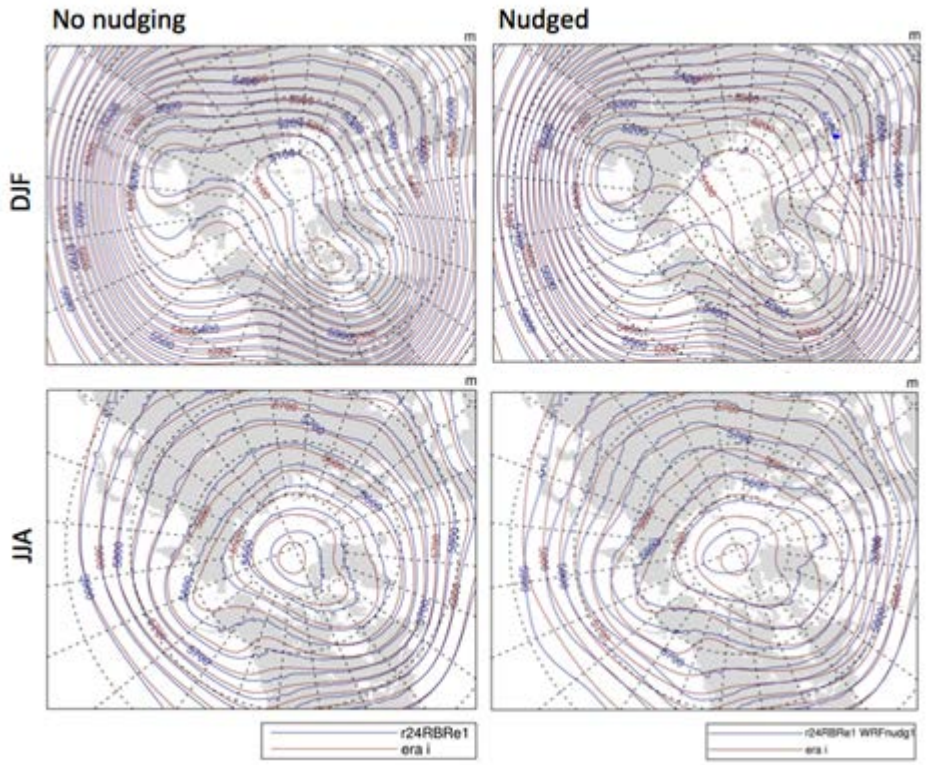

Figure 2. Mean DJF (top) and JJA (bottom) 500 hPA geopotential heights (500 GPH, m) contours in ERA Interim (red contours, all panels), RASM_nonudg (blue contours, left panels), and RASM_nudg (blue contours, right panels).

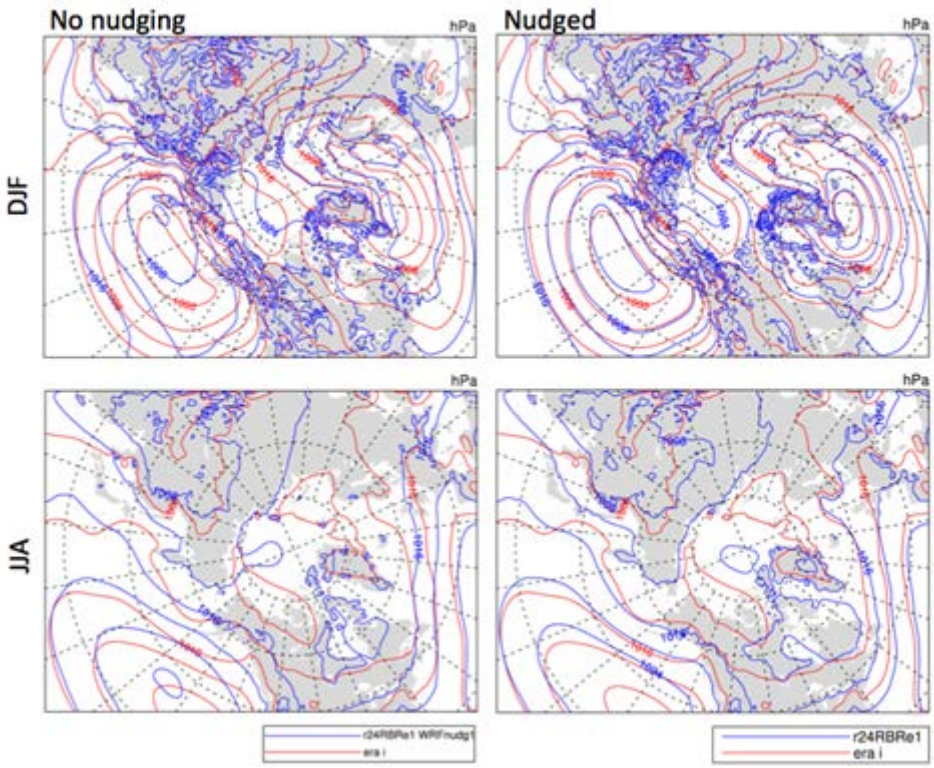

Figure 3. Mean DJF (top) and JJA (bottom) sea level pressure (SLP, hPA) contours in ERA Interim (red contours, all panels), RASM_nonudg (blue contours, left panels), and RASM_nudg (blue contours, right panels).

WRF FDDA nudging's impact on other surface variables is not as consistently positive as its impact on circulation. Surface temperature (Fig. 4) is largely more realistic in RASM_nudg compared to RASM_nonudg, but not at all locations. In winter, RASM_nonudg is much warmer than RASM_nudg in the Canadian Arctic, likely due to greatly decreased (and unrealistic) sea ice in RASM_nonudg. In summer, RASM_nonudg is slightly warmer is most of the domain compared to RASM_nudg, which improves agreement with ERA Interim in regions where RASM has a cold bias (e.g., northeastern Pacific Ocean), but aggravates warm biases in RASM_nudg (e.g., north central Canada). Different components of the RASM surface energy budget averaged over the polar cap (Fig. 5) also show heterogeneous response to nudging. RASM_nonudg tends to have more downward longwave radiation throughout the year and less downward shortwave radiation for months where that is non-zero than RASM_nudg, suggesting that RASM_nonudg is cloudier than RASM_nudg. RASM_nonudg also has substantially more precipitation over the polar cap, and a wet bias compared with ERA Interim, whereas RASM_nudg has a slight dry bias in summer and fall compared with ERA Interim.

In summer, RASM_nonudg is slightly warmer is most of the domain compared to RASM_nudg, which improves agreement with ERA Interim in regions where RASM has a cold bias (e.g., northeastern Pacific Ocean), but aggravates warm biases in RASM_nudg (e.g., north central Canada). Different components of the RASM surface energy budget averaged over the polar cap (Fig. 5) also show heterogeneous response to nudging. RASM_nonudg tends to have more downward longwave radiation

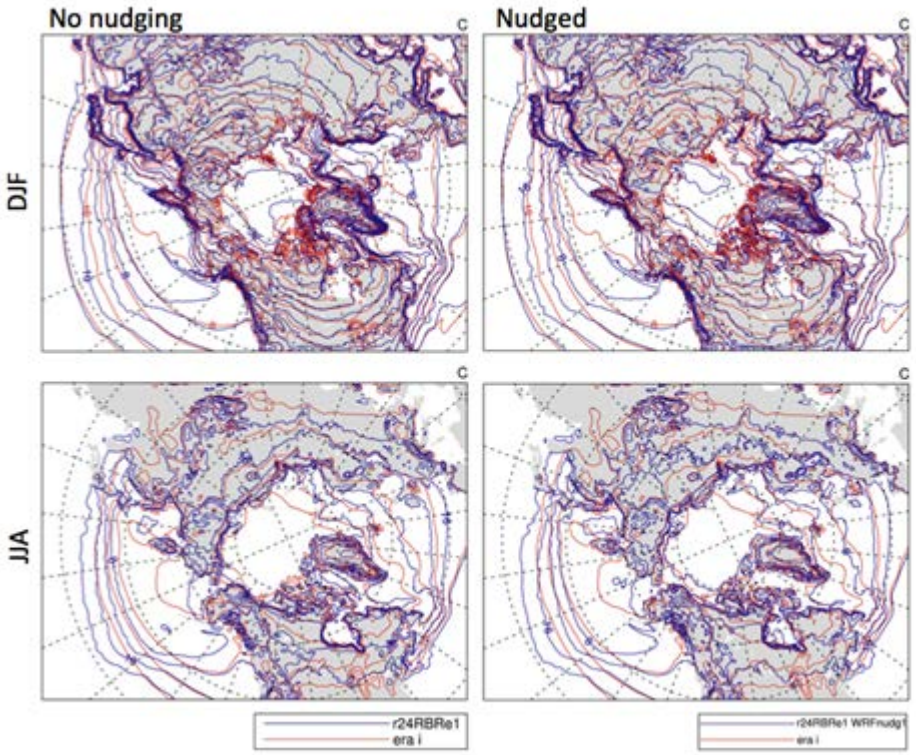

Figure 4. Mean DJF (top) and JJA (bottom) surface temperature (Tsfc, °C) contours in ERA Interim (red contours, all panels), RASM_nonudg (blue contours, left panels), and RASM_nudg (blue contours, right panels).

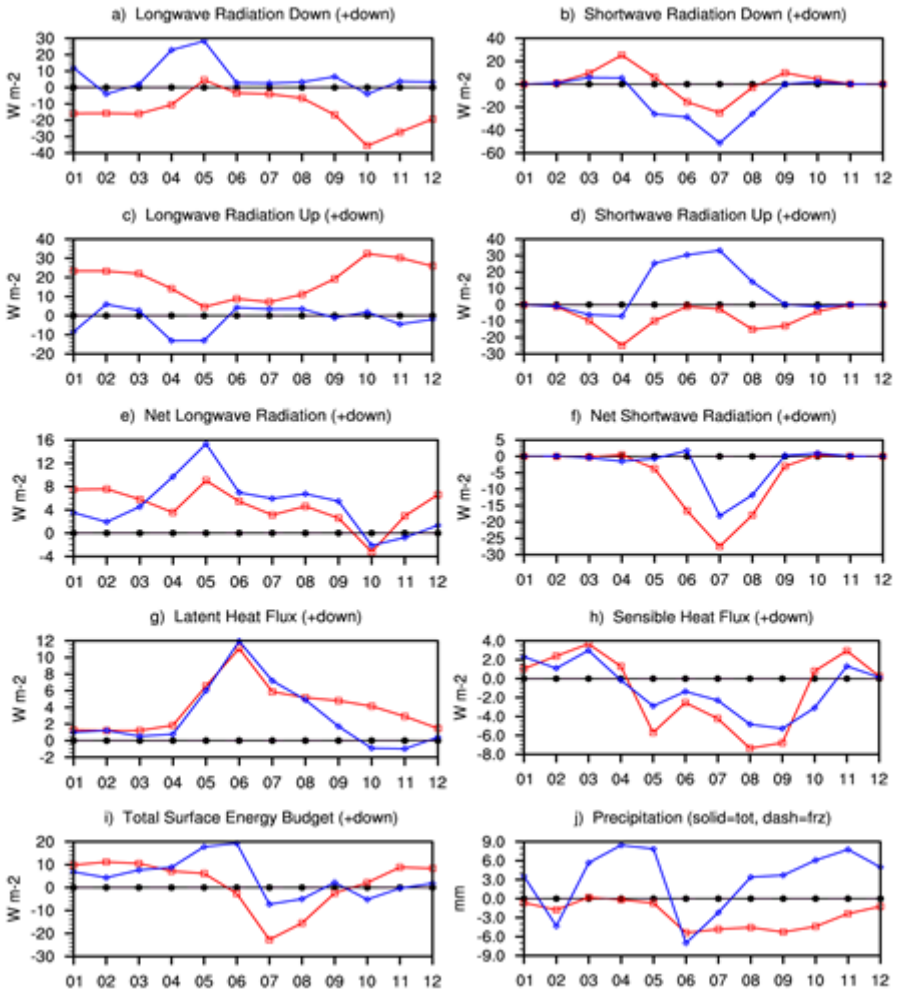

Figure 5. ERA Interim-relative anomalies of polar cap surface energy budget terms as a function of calendar month: (a) downward longwave radiation, (b) downward shortwave radiation down, (c) upward longwave radiation, (d) upward shortwave radiation, (e) net longwave radiation, (f) net shortwave radiation, (g) latent heat flux, (h) sensible heat flux, (i) total surface energy budget, (j) precipitation. Black line shows zero, blue contours show RASM_nonudg anomaly, and red contours show RASM_nudg anomaly.

throughout the year and less downward shortwave radiation for months where that is non-zero than RASM_nudg, suggesting that RASM_nonudg is cloudier than RASM_nudg. RASM_nonudg also has substantially more precipitation over the polar cap, and a wet bias compared with ERA Interim, whereas RASM_nudg has a slight dry bias in summer and fall compared with ERA Interim.

We also completed work during FY14 to configure, compile, and run WRF simulations identical to WRF within RASM, which has undergone many modifications since coupling into RASM and thus differs substantially from WRF 3.2.0 on which it was based. RASM-identical standalone WRF simulations are necessary for this project to document the sensitivity of the coupled system compared to that of the standalone atmosphere.

RASM-CICE sea ice sensitivity to varying parameter space

Sixteen 40-year RASM G-compset runs forced with the Common Ocean Reference Experiment version 2 (CORE2) data for 1970-2009 period were completed to explore CICE model sensitivity to four parameters selected based on their significance with regard to impact on the mean and time varying sea ice states. These parameters include: (i) the ice roughness length scale, which determines the momentum and turbulent heat transfer or the "strength" of ice-atmosphere coupling, (ii) the ice strength, which controls the sea ice response to external and internal dynamic forcing, (iii) the ice-ocean drag coefficient, which is used to compute the ice-ocean stress and indirectly influences the ice-ocean heat flux, and (iv) the ocean vertical mixing parameterization, which contributes to the thermodynamic ice-ocean coupling. Figure 6 shows time series of monthly mean sea ice volume in five sensitivity experiments and model / ICESat Oct-Nov means (Osinski et al. 2014). Figure 7 shows sea ice thickness distribution from four of these experiments.

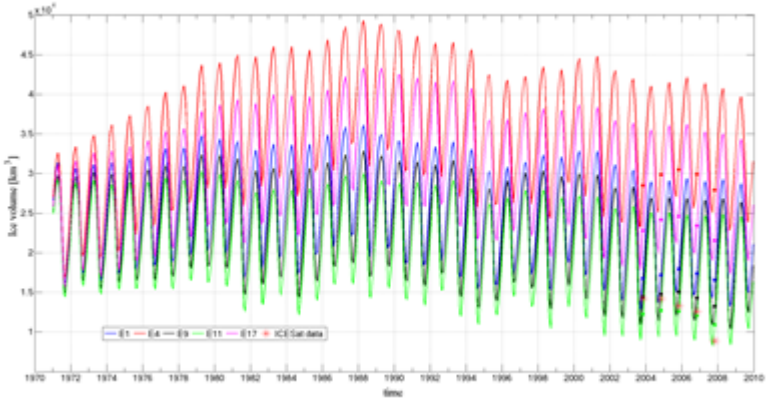

Figure 6. Time series of monthly mean sea ice volume from 5 sensitivity experiments. Oct-Nov mean estimates are shown with red asterisks / color-coded dots from ICESat / model.

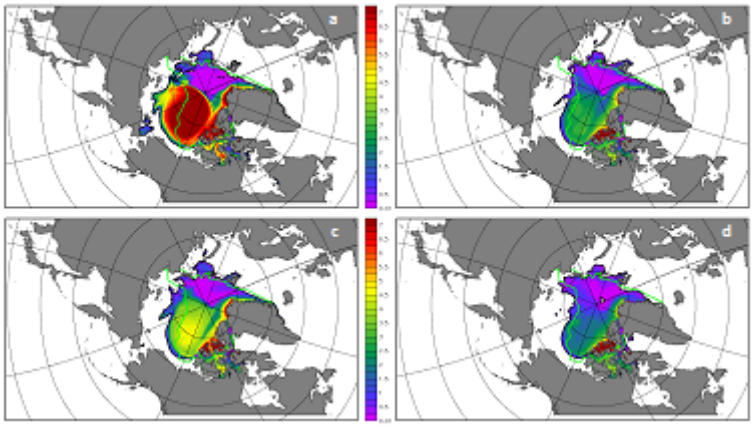

Figure 7. Mean September 2007 ice thickness distribution from 4 sensitivity experiments. The green contour represents the 1979-2009 mean September ice extent from satellites.

Much greater sensitivity to varying parameter space exists in sea ice volume compared to extent as shown in Figures 1 and 2. Our results suggest scale dependence sub-grid scale parameterizations used in climate models, however additional studies are required to properly demonstrate it. More accurate data on sea ice thickness and volume are critical to further constraining model simulation of arctic climate and reducing uncertainty in prediction of its future change scenarios.

Upgrades of RASM-CICE model component

The most important result we would like to report is that RASM now uses anisotropic sea ice mechanics and early results show that this has improved sea ice drift, and most likely thickness, in the model. RASM has been upgraded to Version 5 of the Los Alamos Sea Ice Model (CICE5), and additions and changes to CICE5 resulting from RASM testing are being included in a new public revision of CICE5 at LANL. The physics options now available in RASM's sea ice model include: 1) Anisotropic sea ice mechanics that better simulate oriented linear kinematic features and aligned leads following, Tsamados et al. (2013), otherwise called the Elastic Anisotropic Plastic (EAP) rheology; 2) Form drag that alters both the oceanic and atmospheric neutral drag coefficients of sea ice based on the presents of ridges, melt ponds and level ice as described in Tsamados et al. (2014); 3) A new prognostic salinity thermodynamic model of Turner et al. (2013) that allows progressive draining of brine from the sea ice; and 4) Two new explicit melt pond parameterizations (Flocco et al. 2010; Hunke et al. 2013) better suited to providing summer albedos for WRF for calculating dual-band net downward surface shortwave radiation.

Figure 8 demonstrates the changes to RASM's sea ice thickness and drift when anisotropic rheology is used. This figure includes results using the previous standard rheology in RASM, Elastic Viscous Plastic (EVP; Hunke and Dukowicz 1997) and a recently revised numerical approach to EVP (Revised-EVP; Bouillon et al. 2013). There are stark differences between these three ice mechanics approaches. While Figure 8 qualitatively suggests that the anisotropic rheology may improve central arctic thickness evolution, a comparison of modeled and satellite-derived sea ice drift supports this assertion. Figure 9 is a comparison of the Pathfinder sea ice drift product (Pathfinder; Fowler 2003) with each of the three model rheologies for the winter months when this observational method is most reliable in the central arctic. This comparison represents the first known evaluation of a fully coupled, high-resolution model with anisotropic rheology. The associated sea ice shear for one (December) in Figure 10 illustrates the ability each of the rheologies to generate Linear Kinematic Features (LKFs) akin to those discussed in Kwok et al (2008). As one might expect, the Anisotropic divergence and shear patterns are quite different from both EVP variants, and we will soon begin using RGPS deformation data (e.g. Kwok 2006) to evaluate the realism of each model's LKFs. In understanding the relevance of these results, it is important to understand that there is almost no difference in the surface geostrophic wind that is forcing the sea ice in each case. Therefore all thickness, drift and deformation differences are entirely attributable to sea ice mechanics. Such an assertion is difficult to make in global coupled models, where internal variability typically means that surface geostrophic flow is considerably different between different ensemble members. Conversely, where the same surface geostrophy exists in stand-alone ice-ocean models, they lack coupled feedbacks within the surface boundary layers system.

When our simulations that are currently underway reach the 2000s, we will incorporate ICESat comparisons into the analysis, in the manner indicated in the last year's report. We are also intending to conduct more exacting sea ice drift comparisons against GPS buoy data starting in 1996.

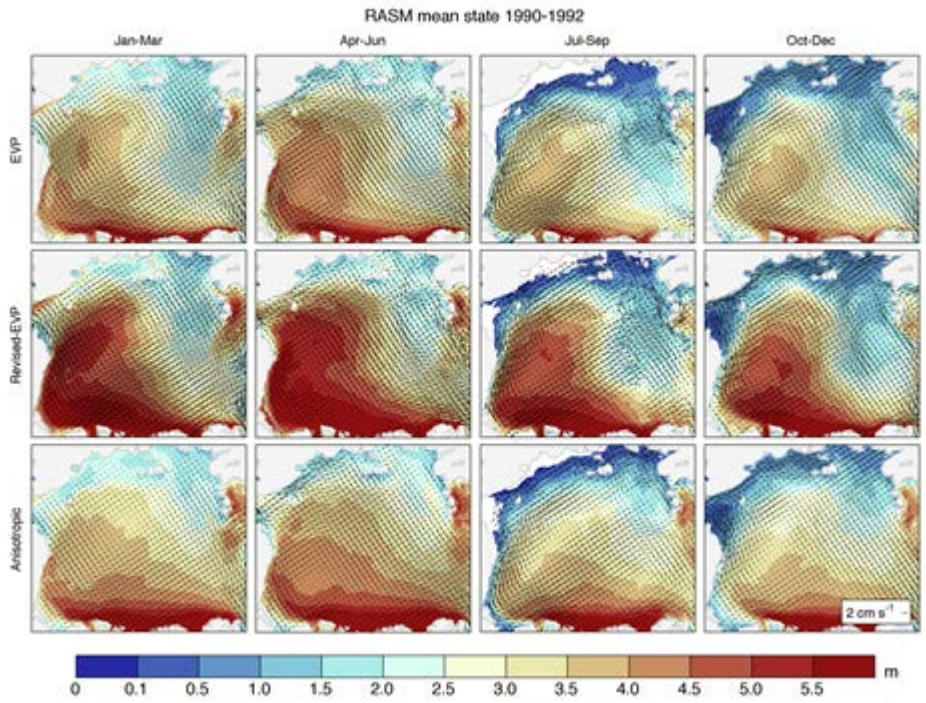

Figure 8. Mean seasonal sea ice thickness, extent and drift for a three year output of the Regional Arctic System Model using three different rheologies: EVP, Revised-EVP and Elastic-Anisotropic-Plastic.

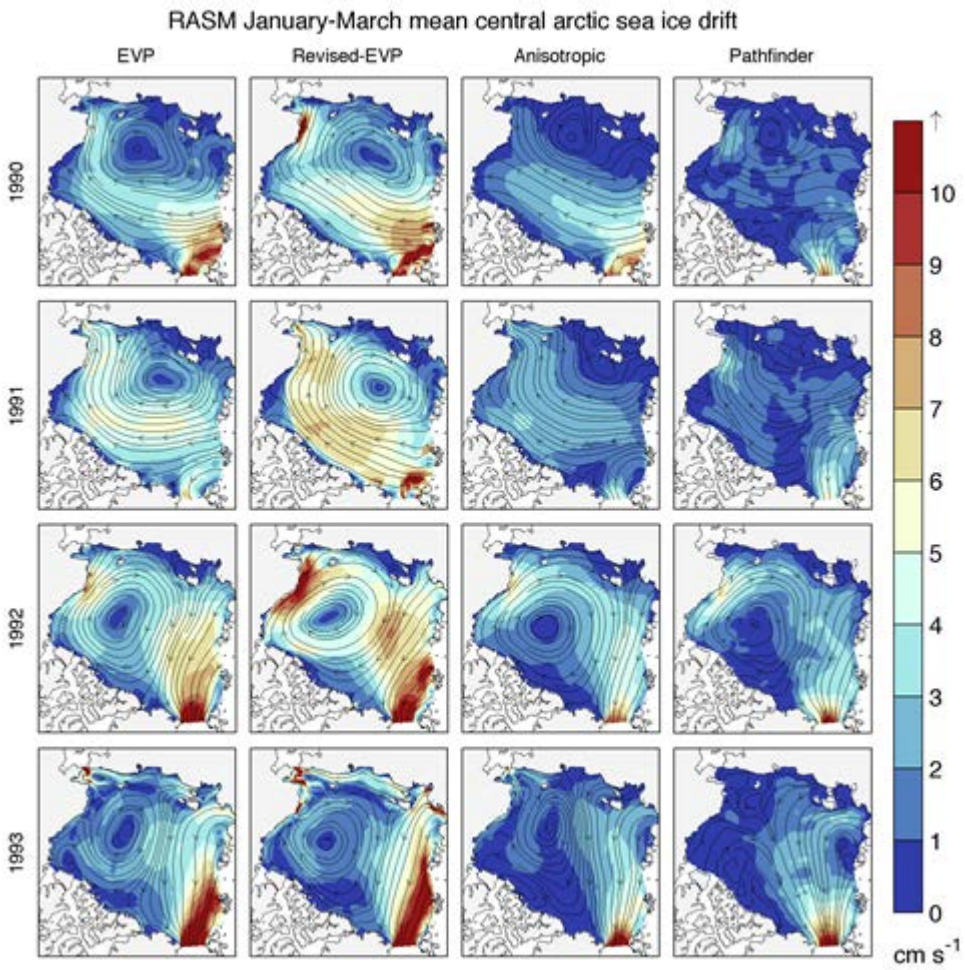

Figure 9. A comparison of mean January-March 1990-1993 central arctic sea ice drift for the three different sea ice rheologies in Figure 8. Observed drift in this instance uses estimates from the Pathfinder dataset (Fowler 2003).

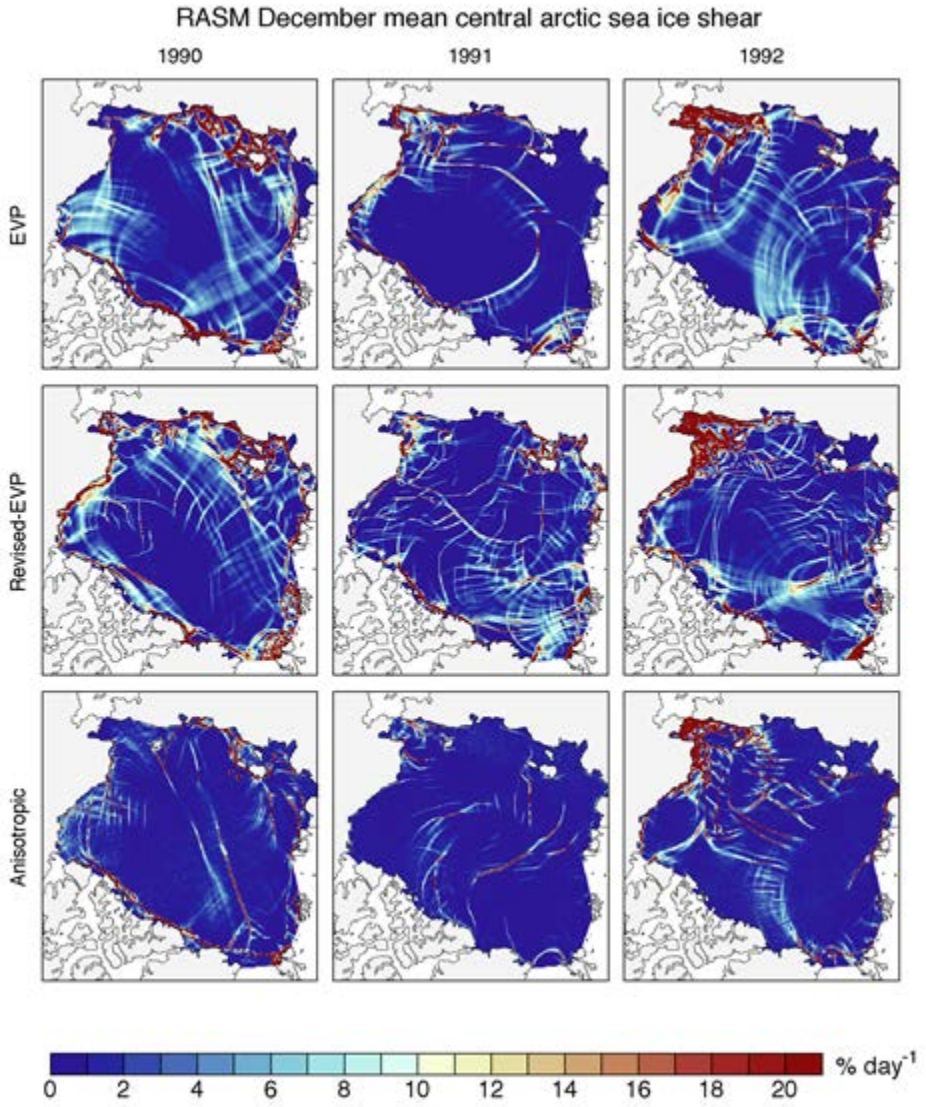

Figure 10. An example of mean sea ice shear during one month for the three different sea ice rheologies in Figure 8. Sharp deformation patterns are equivalent to Linear Kinematic Features observed using the RADARSAT Geophysical Processing System (RGPS).

RASM coupling infrastructure upgrade

There is a fundamental difference between RASM coupling as compared to how many IPCC (2013) models exchange. All RASM model components are coupled at 20-minute intervals, which differs substantially form many other fully coupled models. CESM, for example, coupled the ocean to other components at daily intervals. This latter sampling rate damps near inertial waves in the ice-ocean boundary layer, but more importantly can result in chaotic semi-diurnal motion in the atmosphere. Roberts et al (2014) demonstrate that in using RASM high-frequency ice-ocean coupling, the model is able to replicate observed semi-diurnal motion that is not present in global models, such as CESM. When the RASM coupling infrastructure is applied to CESM, there is a substantial difference in inertial sea ice motion, which can be used as a proxy for ice-ocean Ekman transport. This is illustrated

in Figures 11, where CPL7x represents the RASM-adapted version of the original CESM coupler, CPL7, for high frequency coupling, including important algorithmic changes that obey Hallberg (2014) stability criteria. Although not relevant to this project, the largest difference in the global model when using CPL7x is in fact in the Antarctic (not shown).

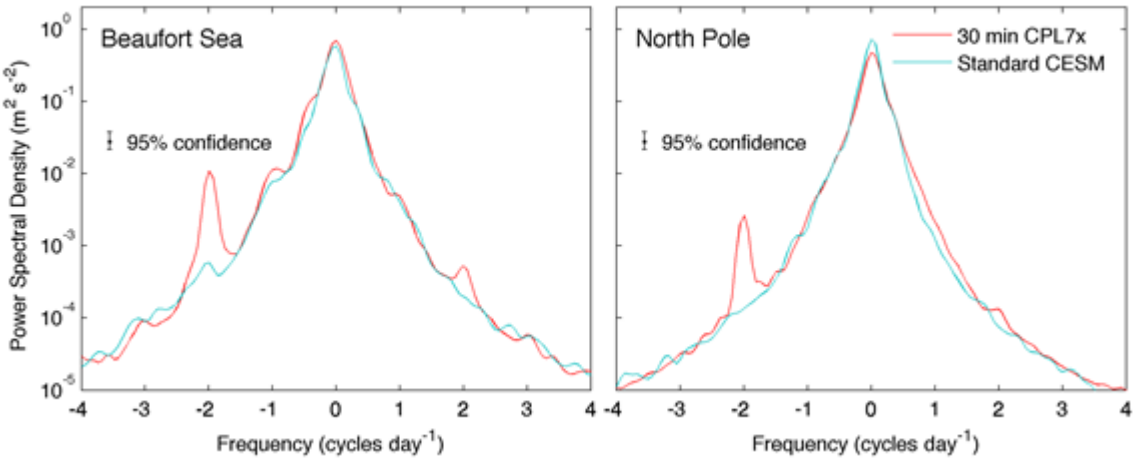

Figure 11. Rotary power spectral density of sea ice drift for a one-year preindustrial simulation of CESM with (red) and without (blue) high-frequency ocean coupling (CPL7x 30 min ocean coupling and CPL7 daily ocean coupling respectively). The peaks at -2 cycles/day represent the inclusion of realistic transient ice-ocean Ekman transport in the model (reproduced from Roberts et al. 2014).

RESULTS

The underlying philosophy of this project is to achieve a realistic, assimilated sea ice state in RASM that is physically consistent across the atmosphere-ice-ocean boundary layer system. Following this strategy, we have made significant progress this year in the sea ice representation of RASM. Our primary focus has been to ensure that upper tropospheric waves are assimilated to the observed planetary scale atmospheric circulation, and under this influence the physics represented in the surface boundary layer system is as realistic as possible. Therefore, our focus in the RASM sea ice model has been to improve the physical representation of processes across the atmosphere-ice-ocean interface, rather than causing physical conflicts in the model, such as momentum leaks, by frequently correcting the sea ice state with direct assimilation of concentration, drift or thickness.

Circulation biases in WRF standalone without nudging are very similar to those in RASM (not shown), suggesting that these biases are almost entirely caused by WRF. Biases in other variables become larger in RASM_nonudg as the simulation integrates longer (not shown), because of the system's (e.g. sea ice) response to the circulation biases. These results suggest that optimally-configured nudging in RASM is imperative to constrain RASM's climate and sea ice evolution. In addition, the tendency for the circulation biases in WRF to be largest at model top is consistent with previous results (e.g. Cassano et al. 2011), and is consistent with both dynamical (e.g., lack of stratospheric dynamics and/or resolution of planetary scale waves in a limited area model) and numerical (e.g., wave reflection at WRF's sponge upper layer) hypothesis for the origin of the biases, which will be explored further in future work.

We find that many parameterizations of subgrid physical processes currently used in climate models need to be optimized and we provide some suggestions on their fine-tuning required when increasing model spatial resolution. We also show that while sea ice extent in many simulations compares well with observations, the model total ice volume only agrees with the limited observational estimates in a few specific cases. Hence, we conclude that the use of observed sea ice extent only to define the skill of sea ice models is not a sufficient constraint.

Within the confines of the RASM model physics, our results suggest scale dependence of some sub-grid scale parameterizations currently used in climate models. However additional sensitivity studies with model configurations at different spatial resolution are required to conclusively demonstrate this point. We expect that a follow on study currently underway with a RASM POP/CICE configuration at $1/48^{o}$, will provide further evidence of scale dependence of some of the parameterizations explored. The presented results from a high-resolution ice-ocean model also point to the need for careful optimization of climate models as we move to process-permitting or process-resolving model configurations, while getting ready for high performance computer capabilities at exascale and beyond.

The ability to test anisotropic mechanics in RASM is important because there has been an ongoing debate in the science community about the relevance of isotropic sea ice mechanics in high-resolution ice-ocean models, which includes the EVP variants presented in this report. RASM resolves the so-called multi-floe scale of 2-10km (McNutt and Overland, 2003), at which it is debatable that sea ice will deform in the same way in all horizontal directions. Observational evidence has long pointed to the tendency for leads to align, further supported by evidence of oriented linear kinematic features (Coon et al. 2007). Isotropic rheologies can mimic this behavior, but the underlying physics are most likely anisotropic. Up to now we have used isotropic mechanics in CICE4. For the first time in a high-resolution fully coupled model, we are able to test for improvements of anisotropy. This now removes that last remaining impediment for us to increase the ice-ocean resolution of RASM to 2.4 km, and we intend to commence these high-resolution simulations in the coming weeks. Papers are underway to demonstrate the advantages of using anisotropic rheology.

Results obtained using RASM CPL7x coupling infrastructure in CESM are important, because they illustrate that many global models are underestimating mixing associated with near-inertial waves, and hence in transferring heat to the underside of sea ice during the passage of storms.

IMPACT/APPLICATIONS

RASM is extensible, and will benefit from the addition of further components, such as a wave model. However, for this project, significant progress can be made using the well tested and working RASM in its current form. Results from this project allow representation of many important processes and feedbacks to understanding past and present states of the Arctic sea ice cover and to reducing uncertainty and improving prediction of its future states.

RASM allows advanced dynamical downscaling of global climate and earth system model future scenarios, including arctic sea ice cover. Such capability is of high interest to the Navy, DOD and U.S. for strategic planning as well as for more detailed information of future climate change impacts in the Arctic. The development of such capabilities is currently actively pursued by the PIs through new competitive research opportunities.

Four NPS USN graduate students have participated in this project under Maslowski's supervision at no cost to this project. Their thesis projects involved analyses of various processes and interactions affecting sea ice cover in the Arctic Ocean as simulated in RASM output. LCDR Mark Murnane, completed research on sea ice kinematics and their impact on ice thickness distribution in the Arctic. LT Thomas Mills focused on evaluating instances of coincident sea ice shear and oceanic upwelling at semi-diurnal frequencies in RASM. Both projects have used high-resolution and/or high-frequency RASM output. LT Dominic DiMaggio completed thesis on the role and variability of ocean heat content in the Arctic Ocean over the period of 1948-2009. Finally, LT James Scianna synthesized multi-decadal variability in the Bering Sea using RASM model results and observations from 1948 to the present.

RELATED PROJECTS

Four complementary projects are of relevance to this project. Two, funded by the DOE/RGCM and DOE/SciDAC programs, involve repectively (i) further expansion of RASM with additional model components for the Greenland Ice Sheet, ice caps, mountain glaciers and dynamic land vegetation and (ii) investigation of the role of mesoscale eddies and tides on ocean circulation and dynamics as well as their contribution of oceanic forcing of sea ice. Two other projects, funded by NSF Office of Polar Programs (NSF/OPP), focus respectively on (i) improved coupling of ice-ocean interface and mixed layer dynamics and their contribution to decadal prediction of sea ice state and climate change in the Arctic and (ii) marine biogeochemistry in the Arctic Ocean and sea ice.

REFERENCES

Bouillon, S., T. Fichefet, V. Legat, and G. Madec (2013), The elastic–viscous–plastic method revisited, Ocean Model., 71, 2–12, doi:10.1016/j.ocemod.2013.05.013.

Bowden, Jared H., Tanya L. Otte, Christopher G. Nolte, Martin J. Otte, 2012: Examining Interior Grid Nudging Techniques Using Two-Way Nesting in the WRF Model for Regional Climate Modeling. J. Climate, 25, 2805–2823. doi: http://dx.doi.org/10.1175/JCLI-D-11-00167.1

Cassano, J. J., M. E. Higgins, and M. W. Seefeldt, 2011: Performance of the Weather Research and Forecasting (WRF) Model for Month-long pan-Arctic Simulations. Mon. Wea. Rev., 139, 3469-3488, doi: 10.1175/MWR-D-10-05065.1.

Comiso, J. (2013), Bootstrap Sea Ice Concentrations from Nimbus-7 SMMR and DMSP SSM/I-SSMIS, 1979-2012. Boulder, Colorado USA: National Snow and Ice Data Center. Digital media.

Coon, M. D., Kwok, R., Levy, G., Pruis, M., Schreyer, H., & Sulsky, D. (2007). Arctic ice dynamics joint experiment (AIDJEX) assumptions revisited and found inadequate. Journal of Geophysical Research-Oceans, 112(C11). doi:10.1029/2005jc003393

Dee, D. P., et al. (2011), The ERA-Interim reanalysis: Configuration and performance of the data assimilation system, Q. J. R. Meteorol. Soc. 137, 553–597.

Flocco, D., D. L. Feltham, and A. K. Turner (2010), Incorporation of a physically based melt pond scheme into the sea ice component of a climate model, J. Geophys. Res., 115(C8), doi:10.1029/2009JC005568.

Fowler, C. (2003), Polar Pathfinder daily 25 km EASE-Grid sea ice motion vectors, http://nsidc.org/data/nsidc-0116.html, Natl. Snow and Ice Data Cent., Boulder, Colo.

Hunke, E. C. and J. K. Dukowicz, (1997), An elastic-viscous-plastic model for sea ice dynamics. J. Phys. Oceanogr., 27, 1849-1867.

Hunke, E. C., D. A. Hebert, and O. Lecomte (2013), Level-ice melt ponds in the Los Alamos sea ice model, CICE, *Ocean Model.*, 71, 26–42.

Kwok, R. (2006). Contrasts in sea ice deformation and production in the Arctic seasonal and perennial ice zones. Journal of Geophysical Research, 111(C11S22). doi:10.1029/2005JC003246

Kwok, R., Hunke, E. C., Maslowski, W., Menemenlis, D., & Zhang, J. (2008). Variability of sea ice simulations assessed with RGPS kinematics. Journal of Geophysical Research-Oceans, 113(C11), -. doi:Artn C11012 Doi 10.1029/2008jc004783

Liu, P.; Tsimpidi, A. P.; Hu, Y.; et al., 2012: Differences between downscaling with spectral and grid nudging using WRF. Atmos. Chem. Phys., 12, 8, 3601-3610. DOI: 10.5194/acp-12-3601-2012.

Maslowski, W., and W. H. Lipscomb, 2003: High resolution simulations of Arctic sea ice, 1979-1993. Polar Research, 22(1), 67-74.

Maslowski, W., J. C. Kinney, M. Higgins, and A. Roberts, 2012. The future of arctic sea ice. Annual Rev. Earth Planet. Sci., 40:625–654.

McNutt, S. L., and J. E. Overland (2003), Spatial hierarchy in Arctic sea ice dynamics, Tellus, 55(A), 181–191.

Osinski, R., W. Maslowski, A. Roberts, J. Clement Kinney, A. Craig (2014), On the sensitivity of sea ice states to variable parameter space in the Regional Arctic System Model, Ann. Glaciol., conditionally accepted.

Roberts, A., A. P. Craig, W. Maslowski, R. Osinski, A. DuVivier, M. Hughes, B. Nijssen, J. Cassano and M. Brunke (2014), Simulating transient ice-ocean Ekman transport in the Regional Arctic System Model and Community Earth System Model, *Ann. Glaciol.*, accepted.

Tsamados, M., D. L. Feltham, and A. V. Wilchinsky (2013), Impact of a new anisotropic rheology on simulations of Arctic sea ice, J. Geophys. Res. Ocean., 118(1), doi:10.1029/2012JC007990.

Tsamados, M., D. L. Feltham, D. Schröder, D. Flocco, S. L. Farrell, N. Kurtz, S. W. Laxon, and S. Bacon (2014), Impact of Variable Atmospheric and Oceanic Form Drag on Simulations of Arctic Sea Ice, J. Phys. Oceanogr., 44(5), 1329–1353, doi:10.1175/JPO-D-13-0215.1.

Turner, A. K., E. C. Hunke, and C. M. Bitz (2013), Two modes of sea-ice gravity drainage: A parameterization for large-scale modeling, J. Geophys. Res. Ocean., 118(5), doi:10.1002/jgrc.20171.